Chemistry & Biology
Article

A Selective Inhibitor of Heme Biosynthesis in Endosymbiotic Bacteria Elicits Antifilarial Activity In Vitro

Christian S. Lentz,[1,3] Victoria Halls,[2,3] Jeffrey S. Hannam,[2] Björn Niebel,[2] Uta Strübing,[1] Günter Mayer,[2] Achim Hoerauf,[1] Michael Famulok,[2,*] and Kenneth M. Pfarr[1,*]
[1]Institute of Medical Microbiology, Immunology and Parasitology, University Hospital Bonn, Sigmund-Freud Strasse 25, 53127 Bonn, Germany
[2]LIMES Institute, Chemical Biology and Medicinal Chemistry Unit, Universität Bonn, Gerhard-Domagk-Strasse 1, 53121 Bonn, Germany
[3]These authors contributed equally to this work
*Correspondence: m.famulok@uni-bonn.de (M.F.), pfarr@microbiology-bonn.de (K.M.P.)
http://dx.doi.org/10.1016/j.chembiol.2012.11.009

SUMMARY

Lymphatic filariasis and onchocerciasis are severe diseases caused by filarial worms and affect more than 150 million people worldwide. Endosymbiotic α-proteobacteria *Wolbachia* are essential for these parasites throughout their life cycle. Using a high-throughput chemical screen, we identified a benzimidazole compound, wALADin1, that selectively targets the δ-aminolevulinic acid dehydratase (ALAD) of *Wolbachia* (wALAD) and exhibits macrofilaricidal effects on *Wolbachia*-containing filarial worms in vitro. wALADin1 is a mixed competitive/noncompetitive inhibitor that interferes with the Mg^{2+}-induced activation of wALAD. This mechanism inherently excludes activity against the Zn^{2+}-dependent human ortholog and might be translatable to Mg^{2+}-responsive orthologs of other bacterial or protozoan pathogens. The specificity profile of wALADin1 derivatives reveals chemical features responsible for inhibitory potency and species selectivity. Our findings validate wALADins as a basis for developing potent leads that meet current requirements for antifilarial drugs.

INTRODUCTION

Lymphatic filariasis and onchocerciasis are vector-borne diseases caused by the filarial nematodes *Wuchereria bancrofti*, *Brugia timori*, *Brugia malayi*, and *Onchocerca volvulus* and are rated as major public health problems by the World Health Organization. More than 1.2 billion inhabitants in endemic countries are at risk of developing the disabling and stigmatizing chronic diseases, i.e., lymphedema and hydrocele in lymphatic filariasis, or severe dermatitis and blindness in onchocerciasis (Hoerauf et al., 2011; Taylor et al., 2010).

Mass drug administration programs (MDA) using annual treatment with a combination therapy of diethylcarbamazine (DEC) or ivermectin (IVM) plus albendazole are used in many endemic countries (Global programme to eliminate lymphatic filariasis, 2009, 2011) to reduce the transmission of filarial disease, mainly by killing offspring microfilariae (MF), and to prevent exacerbation of the disease (Hoerauf et al., 2011; Taylor et al., 2010), while adult worms that persist in the human host for several years are merely paralyzed.

In an environment with increasing reports of suboptimal responses against standard IVM and DEC therapy (Bourguinat et al., 2011; Churcher et al., 2009; Esterre et al., 2001; Osei-Atweneboana et al., 2011) and the exclusion of use of either drug in certain geographical regions due to adverse effects of DEC in onchocerciasis and IVM in loiasis (Gardon et al., 1997), the call for novel antifilarial drugs or treatment options has been raised (Bockarie and Deb, 2010).

As a step toward novel antifilarial pharmacotherapy, the spotlight has turned on endosymbiotic α-proteobacteria, known as *Wolbachia*, that are found in all filarial species causing lymphatic filariasis or onchocerciasis (Taylor et al., 2005). Depletion of prokaryotic *Wolbachia* from its hosts by tetracycline antibiotics leads to sterility of adult worms followed by their death, showing that *Wolbachia* are a target for antifilarial drug design (Hoerauf et al., 2000). However, despite the efficacy of doxycycline with regard to the sterilization of worms, alleviation of pathology, and successful clinical use (Hoerauf et al., 2009), the logistically complicated and expensive treatment regimens and contraindications for large groups in the population prevent its use in MDA (Geary and Mackenzie, 2011; Hoerauf et al., 2009).

In the annotated genome from the *Wolbachia* endosymbiont of *B. malayi*, several essential biochemical pathways such as purine, riboflavin, and heme biosynthesis were identified that are absent or incomplete in the filarial host (Foster et al., 2005; Ghedin et al., 2007) and are considered promising sources of novel targets in antifilarial drug development (Slatko et al., 2010; Wu et al., 2009). A candidate target in *Wolbachia* is δ-aminolevulinic acid dehydratase (wALAD; also known as porphobilinogen [PBG] synthase, E.C. 4.2.1.24, encoded by the *hemB* gene), an enzyme that catalyzes the first common step of tetrapyrrole synthesis—namely, the condensation of two molecules of 5-aminolevulinic acid (5-ALA) to PBG, a function conserved in all organisms that endogenously synthesize heme, chlorophyll, or corrins (Jaffe, 2004).

To explore wALAD as a target for antifilarial therapy, we designed a wALAD activity-based chemical screening assay to

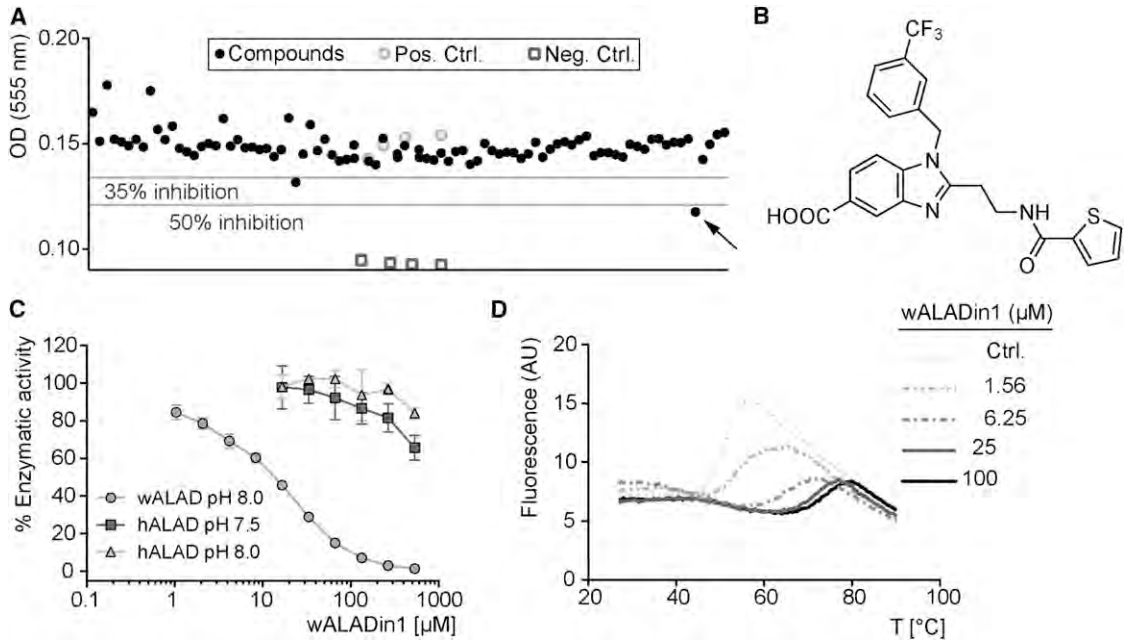

Figure 1. HTS Identifies the Substituted Benzimidazole wALADin1 as a Species-Specific Inhibitor of wALAD

Recombinant wALAD was subjected to HTS ($Z' = 0.65 \pm 0.20$) against a library of ~18,000 small molecules.

(A) One primary screening plate on which the most potent species-selective inhibitor, called wALADin1 (arrow), was detected. Positive control (Pos. Ctrl.) of the enzymatic assay contained protein, substrate, and 6.7% DMSO; for negative control (Neg. Ctrl.), substrate was omitted.

(B) Chemical structure of wALADin1.

(C) Dose-response curve for wALADin1 incubated with wALAD and hALAD revealing species-selective inhibition wALAD (IC_{50}, ~11 μM at pH 8.0). hALAD is only marginally affected (IC_{50} > 500 μM for pH 7.5; IC_{50} > 1 mM for pH 8.0). The graph is representative of three experiments showing mean ± SD.

(D) Melting curve of 5 μM wALAD measured as an increase in fluorescence intensity of the environmentally sensitive dye SYPRO Orange; increasing concentrations of wALADin1 stabilized wALAD tertiary structure (rightward shift of the melting curves).

See also Figure S1 and Table S1.

identify wALAD inhibitors from a library of ~18,000 drug-like compounds. Here, we report the discovery of a class of substituted benzimidazole-5-carboxylic acid structures, called wALADins, as species-selective inhibitors of wALAD that show only negligible inhibition of the human ortholog. We demonstrate macrofilaricidal effects of wALADin1 in *Wolbachia*-containing filarial worms in an ex vivo culture system, a finding that will allow the exploitation of this exciting class of wALAD inhibitors for the future development of potent antifilarial leads for drugs that might eradicate lymphatic filariasis and onchocerciasis.

RESULTS

Identification of a Specific wALAD Inhibitor

We established a high-throughput screening (HTS)-compatible assay by monitoring the wALAD-catalyzed conversion of 5-ALA to PBG, the formation of which was detected by a colored condensation product with *p*-dimethylamino-benzaldehyde (Ehrlich's Reagent) at 555 nm (see a detailed overview of the HTS assay in Table S1 available online). A chemical library containing ~18,000 diversity-based drug-like small molecules (Hafner et al., 2006, 2008; Niebel et al., 2010; Yamazaki et al., 2007) was screened to identify inhibitors of wALAD. The average assay quality parameter Z' was 0.65 ± 0.20 throughout the screening, indicating robust assay performance (Figure 1A).

The screening revealed a cluster of substituted benzimidazole derivatives that inhibited wALAD activity in a dose-dependent manner, while activity of the human ortholog hALAD was only marginally affected. The most potent of these compounds was termed wALADin1 **1** (*wolbachia* ALAD inhibitor **1**) (Figure 1B). It inhibited wALAD with a half maximal inhibitory concentration (IC_{50}) of ~11 μM compared to an extrapolated IC_{50} of ~740 μM for hALAD (Figure 1C). hALAD remained unaffected by wALADin1 both at pH 8, the pH optimum of wALAD, and at pH 7.5, which is within the hALAD optimal pH range. The >60-fold discrimination in inhibitory potency of the endobacterial over the human ALAD ortholog indicates that wALADin1 is a species-selective inhibitor.

We next performed thermal shift assays to demonstrate that wALADin1 binds to wALAD. As hydrophobic side chains become exposed upon thermal denaturation, the melting curve of a protein can be measured as an increase in fluorescence intensity of the environmentally sensitive fluorescent dye Sypro Orange (Zhang and Monsma, 2010). Increasing concentrations of wALADin1 in the low micromolar range led to a concentration-dependent rightward shift of the melting curve consistent with stabilization of the protein by ligand binding under enzymatic assay buffer conditions (Figure 1D). For hALAD, only concentrations of wALADin1 ≥250 μM led to a slight shift of the melting temperature, but ΔT_m values did not exceed 1.5°C at 1 mM (Figure S1A). wALADin1 did not interact with other

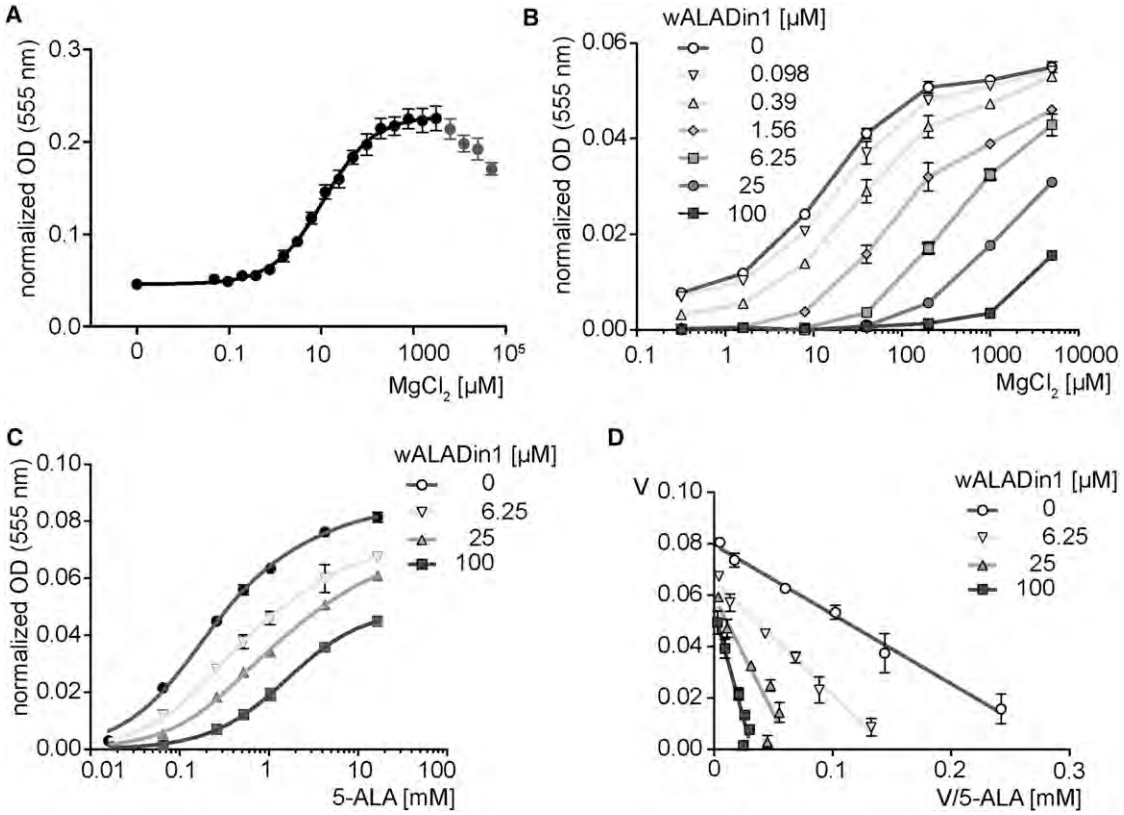

Figure 2. wALADin1 Functionally Competes with Enzymatic Activation by Mg^{2+} and Acts by Mixed Competitive, Noncompetitive Inhibition

(A) wALAD activity is Mg^{2+} responsive (EC_{50} = 11 μM; near-saturating 5-ALA concentration of 1 mM). Graph depicts mean ± SEM of three experiments.

(B) Mg-response curve of wALAD (non-saturating 5-ALA concentration of 200 μM) is shifted to the right by increasing concentrations of wALADin1

(C) 5-ALA serial dilutions in the presence of different concentrations of wALADin1. Lines were fitted to a double hyperbole (Prism 5.0) accounting for different oligomeric structures with different activities (R^2 = 0.99902–0.9961).

(D) Linearized Eadie-Hofstee representation revealing reduced V_{max} and increased K_M upon inhibition with wALADin1.

(B), (C), and (D) show means ± SD of two experiments.

See also Figure S2.

control proteins (bovine serum albumin [BSA], lysozyme). (Figures S1B and S1C). These experiments demonstrate that wALADin1 specifically binds to wALAD.

wALADin1 Interferes with wALAD Activation by Mg^{2+}

Having qualitatively described the binding between wALADin1 and its enzymatic target, we characterized this inhibitor in terms of its molecular mode of action. As wALAD is a Mg^{2+}-responsive enzyme (EC_{50}, ~11 μM, Figure 2A), we studied the influence of Mg^{2+} concentration on the inhibitory properties of wALADin1. The observed rightward shift of the Mg^{2+} response curve in the presence of increasing concentrations of wALADin1 indicates a functional competition between inhibition by wALADin1 and the activation induced by Mg^{2+} (Figure 2B).

We then determined the underlying type of inhibition by measuring enzymatic activity at different wALADin1 concentrations with varying concentrations of the 5-ALA substrate. δ-aminolevulinic acid dehydratase (ALAD) proteins are morpheeins that can form multiple homomeric assemblies that show dramatic differences in their catalytic activities (Jaffe, 2005; Lawrence et al., 2008). Nonlinear regression analysis (NLR) assuming a double hyperbolic progression representing different V_{max} and K_M values of different oligomeric assemblies of the morpheein (with high affinity and activity for an octameric and reduced affinity for lower molecular weight assemblies) gave the best fits (R^2 values, 0.9902–0.9961). An increase in both apparent K_M values and a reduction in the overall V_{max} in the presence of increasing 5-ALA concentrations was observed (at 6.7% dimethyl sulfoxide [DMSO]: V_{max1} = 0.071, K_{M1} = 163 μM, V_{max2} = 0.014, and K_{M2} = 3.4 mM; at 25 μM wALADin1: V_{max1} = 0.046, K_{M1} = 456 μM, V_{max2} = 0.023, and K_{M2} = 6.4 mM). For 100 μM wALADin1, a double hyperbolic fit was not superior to a simple hyperbole (V_{max} = 0.049, K_M = 1.6 mM). The inhibitory mechanism predicted by NLR data is consistent with the linearized Eadie-Hofstee representation suggesting a mixed competitive/noncompetitive mode of inhibition (Figures 2C and 2D). NLR assuming classic mixed model inhibition had a slightly poorer fit but was useful for approximation of the inhibition constant K_i of 5.95 ± 0.95 μM (α = 31.44 ± 9.59; R^2 = 0.9794) at 1.0 mM $MgCl_2$.

For pea and human ALAD compounds that stabilize the inactive hexameric over the active octameric, conformation elicited ortholog-specific inhibition. Native PAGE analysis of wALAD, with hALAD used as controls for the localization of hexameric

and octameric bands (Figure S2A), revealed that preincubation with wALADin1 did not alter the oligomeric equilibrium but it bound to and reduced activity of wALAD octamers in an in-gel activity assay (Figure S2B).

wALADin1 Elicits Filaricidal Activity in Worms Containing *Wolbachia*

Having characterized the inhibitory effects of wALADin1 on wALAD at the molecular level, we proceeded to demonstrate its antifilarial activity. We therefore tested wALADin1 against the rodent filarial nematode *Litomosoides sigmodontis* (*Ls*), a model for human filarial nematodes causing lymphatic filariasis and onchocerciasis that also harbors *Wolbachia* endobacteria (Hoerauf et al., 1999). wALADin1 was tested against *Ls* in a coculture assay with monkey kidney LLC-MK2 feeder cells within a concentration range between 125 and 500 μM. These levels exceeded the IC_{50} concentration of the enzymatic assay by ~10-fold to ~50-fold—an excess we expected to be required to achieve near-complete inhibition in the living worm. Indeed, we observed a concentration- and time-dependent decrease in motility of adult *Ls* females for all concentrations tested in the course of the 17-day culture period (Figure 3B).

Healthy worms make very quick, fidgeting continuous movements over their entire body length. The phenotype of wALADin1-treated worms had a specific and characteristic appearance: the worms first formed slowly moving ball- or knot-like shapes (rated with a motility score of 4) that later became largely immotile (score of 3). This phenotype preceded the stretched low-motility forms that characterized the phenotype of dying worms (Figure 3A; Movies S1, S2, S3, S4, and S5). The pronounced filaricidal effect of wALADin1 was consistent for all concentrations tested as quantified in a viability measurement (MTT assay; Mann-Whitney U test, $p < 0.05$) (Figure 3C). Median viability was reduced to 44%, 27%, or 7.5% (normalized to 1% DMSO groups as 100% viability and dead control group set to 0%) by 125 μM, 250 μM, or 500 μM, respectively, suggesting an IC_{50} concentration of ~100 μM in this assay.

We complemented these studies with cytotoxicity experiments using wALADin1 on both LLC-MK2 (monkey kidney) cells and human embryonic kidney (HEK) cells. Viability of the cells was measured by MTT assay after 48 hr incubation at different concentrations of wALADin1. Viability was reduced for both cell lines at 500 μM and 1 mM wALADin1 (Figure S3A). However, at 500 μM. the LLC-MK2 cell lawn in the worm coculture was always intact, and cells showed no sign of apoptosis. Thus, the observed effect on viability at that concentration may be attributed to an antiproliferative activity of wALADin1 rather than cytotoxicity.

To dissect the contributions of nonspecific cytotoxic and specific antifilarial effects resulting from ALAD inhibition in the *Wolbachia* endosymbionts of *Ls* worms, we tested wALADin1 against *A. viteae* (*Av*), another model rodent filarial nematode that does not have *Wolbachia* (Hoerauf et al., 1999). We performed a nucleotide query of the recently completed *Av* genome database (Blaxter, 2012) using the *hemB* genes (that code for ALAD) of *Wolbachia* of *B. malayi*, human, and yeast as input sequences (accession number AE017321.1, gene locus Wbm0373; X64467; J03493) that showed that there are no orthologous genes in this worm. Therefore *Av* should only be sensitive to nonspecific cytotoxic effects of the compounds. Exposure to 500 μM wALADin1 had an effect, reducing *Av* motility to a score of 4 within 2 hr, and motility remained at this level for ~10 days (Figure 3D). However, there was no significant influence on the viability of *Av* worms in the more accurate MTT assay (Figure 3E). Note that direct comparison of motility scores between *Ls* and *Av* is restricted by their different motility phenotypes (*Av* worms move more slowly) (Supplemental Experimental Procedures; Movies S1, S2, S3, S4, and S5). The characteristic balled phenotype observed in wALADin1-treated *Ls* was absent in *Av*. At wALADin1-concentrations lower than 500 μM, neither an effect on viability nor one on motility of *Av* was detectable, whereas a >50% impairment of viability on *Ls* was seen already at 125 μM. Taken together, the antifilarial effect of wALADin1 on *Ls* is thus due to the dependence of this species on *Wolbachia*.

The antifilarial effect of wALADin1 might be enhanced by a combination of reduced heme levels and excess 5-ALA-induced toxicity, as 5-ALA levels are expected to build up as a consequence of ALAD inhibition. In order to verify this hypothesis, motility and viability of *Ls* as a function of 5-ALA concentration were assessed. Both parameters were reduced upon treatment with 1 or 5 mM 5-ALA (Figures S4A and S4B). Thus, exposure to increased 5-ALA levels indeed has a filaricidal effect.

Specificity of wALAD Inhibitors

The antifilarial activity and the species selectivity of wALAD inhibition encouraged us to characterize in greater depth the activity and specificity of wALADin1 **1** (all compounds are continuously numbered and are referred to as bold numbers **1**–**16**). We first assessed the general influence of single substituent groups R^1, R^2, and R^3 present in the benzimidazole scaffold of **1** on the overall inhibitory activity by successively replacing each group with a hydrogen atom (Compounds **2**, **3**, and **4**) (Table 1). Compound **3** retained the inhibitory potency of wALADin1 indicating that the 2-[(2-thienylcarbonyl)amino]ethyl residue of **1** is dispensable for inhibitory activity. In contrast, the absence of the R^1 3-CF_3 benzyl group (**2**) or the R^3-COOH function (**4**) led to an abrogation of inhibitory activity. A methyl ester variant of **1**, compound **5**, was equally inactive as **4**, revealing the importance of the carboxyl group for wALAD inhibition: either the solubility of the compounds is affected in a way that prevents inhibitory potency, or the carboxylic acid moiety is functionally required. To test this, we performed a carboxylate scan by attaching the COOH-group at benzimidazole atoms C_6, C_4, and C_7 (**6**, **7**, and **8**, respectively). While **7** was inactive, **6** and **8** showed a 29-fold and 15-fold loss of inhibitory potency, respectively, indicating that activity is affected by the positioning of the carboxy group rather than solubility.

Isomers **6**–**8** were also tested in the thermal shift assay for wALAD binding. The noninhibitory compound **7** does not stabilize wALAD at all, whereas **6** and **8** stabilize the protein with discernible but smaller melting shifts (ΔT_m) than wALADin1 (Figure S1), which is commonly interpreted as reduced binding affinities (Zhang and Monsma, 2010). These results concur with the IC_{50} values determined in the enzymatic inhibition data. Different entropic and enthalpic contributions to the free energy of binding between **6** and **8** may explain the considerably larger ΔT_m of **6**,

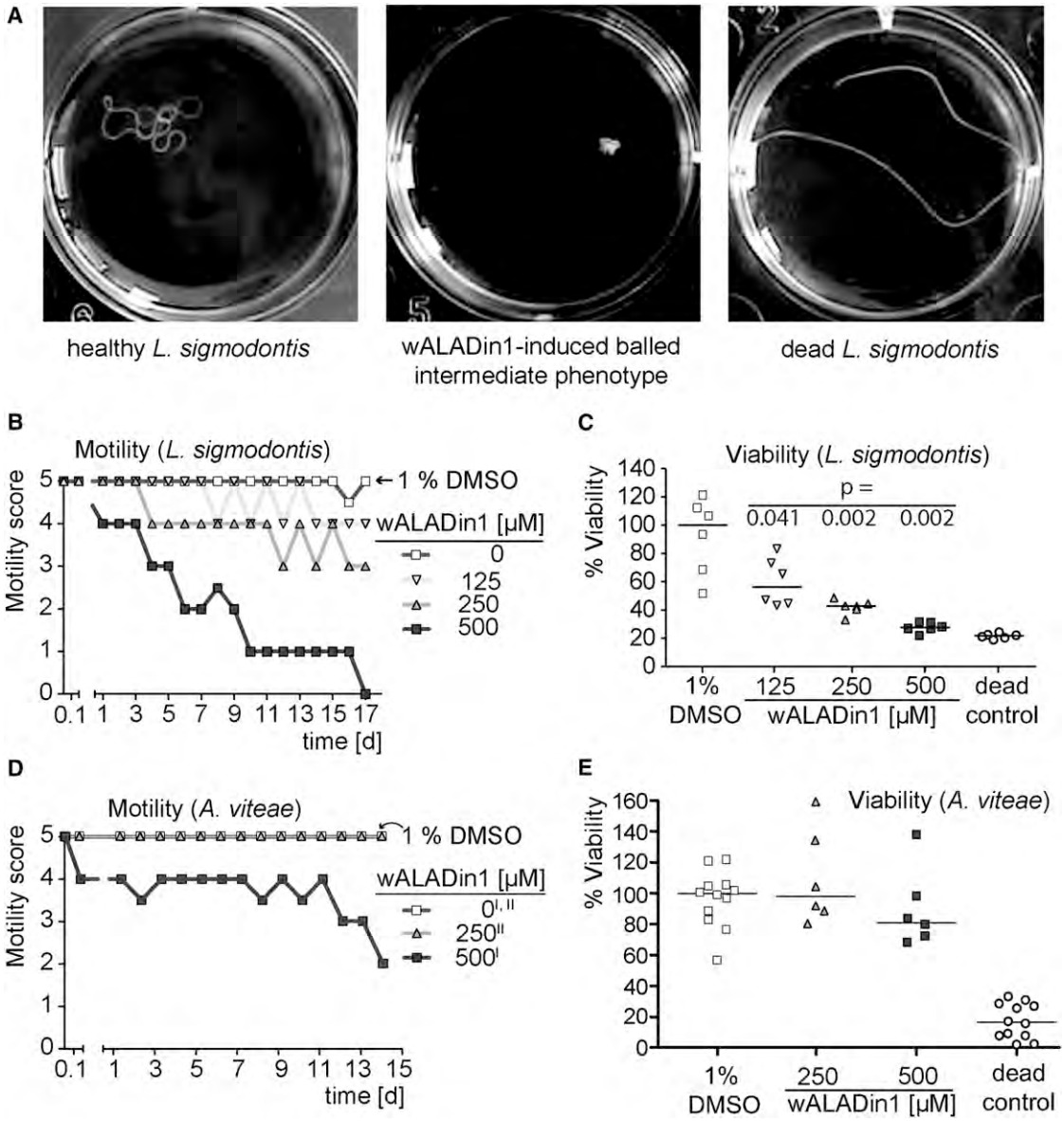

Figure 3. wALADin1 Has a *Wolbachia*-Dependent Macrofilaricidal Activity In Vitro

(A) Pictures of female *Ls* adult worms showing different phenotypes seen in the course of wALADin1 treatment.

(B–E) Survival assays with the *Wolbachia*-containing filaria *Ls* in (B) and (C) and the *Wolbachia*-devoid control filaria *Av* in (D) and (E) with wALADin1. Worms were cultivated until single 1% DMSO-treated control worms began to lose motility (14–17 days). (B) Motility of *Ls* and (D) *Av* worms treated with wALADin1 or 1% DMSO were rated visually as described in the Supplemental Experimental Procedures. Motility graphs show median values (n = 6). Worm viability was measured by MTT assay at the end of treatment for *Ls* (C) and *Av* (E). Optical density (OD) data were normalized to the 1% DMSO control (100% viability), and dead (frozen + boiled) worms were used as negative control. Data are representative of two experiments. Significance was tested by nonparametric two-tailed Mann-Whitney U test; significant p values are depicted in the graph. For *Av*, data of two independent experiments are shown marked with superscript I and II in (D); for normalized viability data, control worms from both experiments were pooled in (E). d, days.

See also Figures S3 and S4 and Movies S1, S2, S3, S4, and S5.

being the slightly less potent inhibitor. Overall, these results demonstrate that the position of the carboxylic acid at the benzimidazole ring is crucial for the inhibitory potency and indicate an involvement of this group in binding, e.g., by salt bridge formation.

Alterations of the R^1-substituent generally led to a decrease in inhibitory activity. For example, moving the CF_3 group in the R^1-isomer of wALADin1 from position 3 (**1**) to position 4 (**9**) resulted in a 4-fold reduced activity. As R^2 is apparently dispensable for inhibition, we synthesized a series of R^1-variants with an R^2-H substituent. Interestingly, compound **10**, the R^2-H derivative of compound **9** was ~2-fold less active (IC_{50} ~88 µM) than **9**, indicating R^2-substituents may confer additional potency. Compared to **3**, the re-positioning of the CF_3 residue in R^1 (**10**) or

Table 1. IC_{50} Values Obtained for the Inhibition of wALAD and hALAD by wALADin1 and Derivatives under Standard Conditions

Compound	R_1 Residue	R_2 Residue	R_3 Residue	R_3 Position at Benzimidazole	*Wolbachia* ALAD		Human ALAD	
					IC_{50} (μM)	R^2	IC_{50} (μM)	R^2
1	3-trifluoromethyl benzyl	2-[(2-thienylcarbonyl)amino]ethyl	−COOH	C_5	11.1 ± 1.0	0.9517	*~739 ± 103*	*0.8582*
2	−H	2-[(2-thienylcarbonyl)amino]ethyl	−COOH	C_5	*	–	*	–
3	3-trifluoromethyl benzyl	−H	−COOH	C_5	13.0 ± 1.2	0.9638	197 ± 20	0.9457
4	3-trifluoromethyl benzyl	2-[(2-thienylcarbonyl)amino]ethyl	−H	C_5	*	–	*	–
5	3-trifluoromethyl benzyl	2-[(2-thienylcarbonyl)amino]ethyl	$-COOCH_3$	C_5	*	–	*	–
6	3-trifluoromethyl benzyl	2-[(2-thienylcarbonyl)amino]ethyl	−COOH	C_6	317 ± 53	0.9022	*	–
7	3-trifluoromethyl benzyl	2-[(2-thienylcarbonyl)amino]ethyl	−COOH	C_4	*	–	*	–
8	3-trifluoromethyl benzyl	2-[(2-thienylcarbonyl)amino]ethyl	−COOH	C_7	164 ± 14	0.9551	*	–
9	4-trifluoromethyl benzyl	2-[(2-thienylcarbonyl)amino]ethyl	−COOH	C_5	38.6 ± 6.2	0.9670	*~618 ± 105*	*0.9186*
10	4-trifluoromethyl benzyl	−H	−COOH	C_5	87.7 ± 10.5	0.9487	173 ± 12	0.9730
11	2-trifluoromethyl benzyl	−H	−COOH	C_5	293 ± 67	0.8503	145 ± 7.2	0.9854
12	benzyl	−H	−COOH	C_5	197 ± 33	0.9042	213 ± 6.3	0.9934
13	3-methyl benzyl	−H	−COOH	C_5	134 ± 17	0.9394	222 ± 11	0.9864
14	3-methyl benzyl	−H	−COOH	C_5	205 ± 12	0.9922	156 ± 7.8	0.9881
15	$-CH_3$	−H	−COOH	C_5	*	–	*	–
16	−H	−H	−COOH	C_5	*	–	511 ± 36	0.9780

The results of two independent experiments were pooled for each compound. Compounds were tested in a 2-fold dilution row, with the highest concentration tested being 533 μM. Where low inhibition (<50%) was observed at the highest concentration tested, extrapolated IC_{50} values are shown in italics. Asterisks indicate the absence of inhibitory activity.
See also Figure S1.

its change to CH_3 (**13**) led to 8- and 10- fold reduced potency. As further R^1 substitutions also led to a significant reduction (**11–14**) or abrogation of inhibitory activity (**15, 16**) we conclude that R^1 in general and its CF_3 group in particular are important for inhibitory potential so that the 3- CF_3 benzyl residue is optimal among the series of compounds tested.

It is intriguing that all compounds featuring the 2-[(2-thienylcarbonyl)amino]ethyl at R^2 (**1, 4–9**) are, at best, only very weak inhibitors of hALAD (≥618 μM). In contrast, smaller R^2-H compounds (**3, 10–14**) have IC_{50} values between 145 and 222 μM for hALAD with compounds **11** and **14** being even more potent inhibitors of the human than of the *Wolbachia* protein. These data are summarized in Figure 4 and suggest that, although the R^2–substituent of wALADin1 is not required for inhibiting wALAD, it is important for species selectivity, e.g., by imposing a steric hindrance for the hALAD binding site. Despite the reduction in species selectivity, removal of the R^2-2-[(2-thienylcarbonyl)amino]ethyl group of the 473.5 Da molecule wALADin1 resulting in **3** showed no loss of inhibitory activity and presents the smaller 320 Da compound **3** as an improved lead candidate.

In order to determine the antifilarial profile of wALADin1 derivatives, selected compounds **3** (despite its reduced species selectivity) and **6,** neither of which was cytotoxic at 500 μM (Figure S3B), were tested for antifilarial activity against *Ls* (Figure 5) in the ex vivo culture. Generally, the potent wALAD inhibitor **3** shows similar but slightly less potent antifilarial activity on *Ls* compared to wALADin1, and it also induced the balled phenotype described earlier (Movies S1, S2, S3, S4, and S5). Motility levels only became comparable to those induced by wALADin1 during the last days (scores 3 and 4 for 125 and 250 μM, respectively). Viability was significantly reduced at 500 μM for **3** (38% median residual viability), but the trend continued for the lower doses.

The 500 μM compound **6,** a less potent inhibitor that was still able to bind to wALAD, showed less antifilarial potency than wALADin1 but was stronger than **3**, with *Ls* viability reduced to 24%. The decrease may be related to the rapid, non-ALAD/*Wolbachia*-dependent activity seen in *Av* treated with 500 μM wALADin1 (Figure 3D). Taken together, the structural information of the tested benzimidazole compounds and the pronounced antifilarial activity in vitro observed for the two most potent wALAD inhibitors (wALADin1 and **3**) provides an excellent starting point for the development of a more potent lead structure that targets *Wolbachia* by the specific Mg^{2+}-dependent mode of action we have described herein.

DISCUSSION

Current antifilarial drug discovery strategies follow different approaches: the worms may be targeted directly at nematode proteins, e.g., involved in specific processes such as molting (Gloeckner et al., 2010), or indirectly by killing their *Wolbachia* endosymbionts. Whole-organism-screening approaches are being carried out for both organisms to identify novel antifilarial and anti-*Wolbachia* compounds and drug targets (Serbus et al., 2012). *Wolbachia*-targeting drugs acting like classic antibiotics usually deplete the endobacteria from their hosts (Hoerauf et al., 1999). In this study, we targeted a single biochemical pathway considered essential for symbiosis and maintaining worm homeostasis and that may therefore affect the worm directly and more rapidly than *Wolbachia*-depleting drugs do. The pathway we address is heme biosynthesis, and the target enzyme is wALAD. As *B. malayi* worms only possess the gene

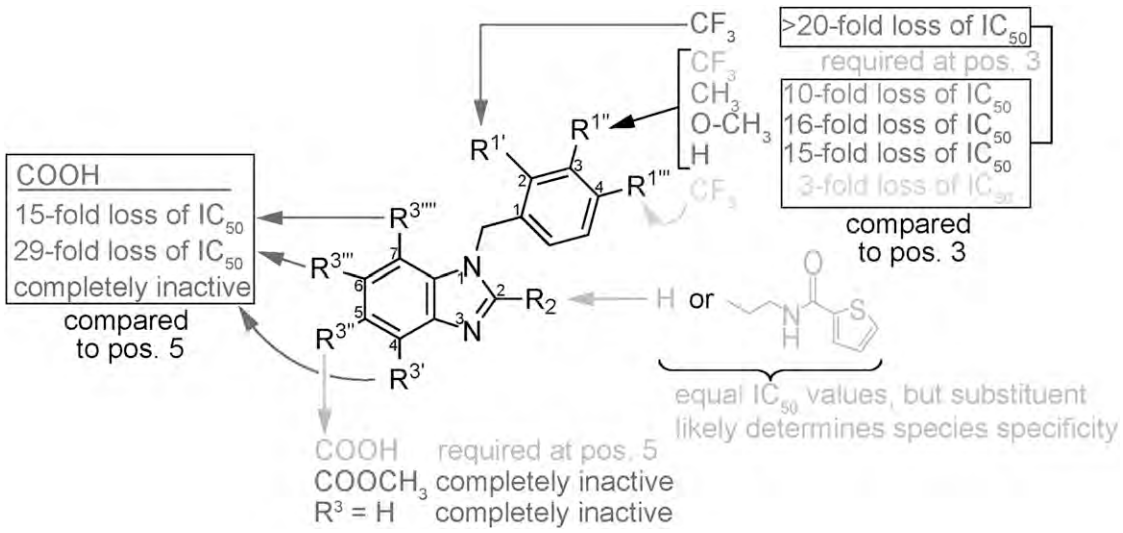

Figure 4. Summary of Activity Data for wALAD Inhibition by wALADin Inhibitors

The R^3-COOH residue is an explicit requirement for inhibitory function and may be involved in salt-bridge formation in the binding site. R^1 is important for inhibitory activity, as all substitutions of the 3-CF_3-methyl benzyl provoked, reduced, or annihilated inhibitory potency with a benzyl group as a minimum requirement. The R^2-2-[(2-thienylcarbonyl)amino]ethyl group of wALADin1 appears to be a major mediator of species selectivity. pos., position.

for ferrochelatase, the last enzyme of heme biosynthesis, and as they are apparently unable to salvage heme from their environment in vitro, they are expected to depend on their endosymbionts that possess the genes required for de novo heme biosynthesis (Foster et al., 2005; Ghedin et al., 2007; Wu et al., 2009).

In contrast, the free-living nematode *Caenorhabditis elegans* is unable to synthesize heme de novo but relies on exogenous heme sources it may exploit via a system of heme transporters (Chen et al., 2012). It is interesting that non-*Wolbachia* carrying filarial nematodes such as *Av* and *L. loa*, the genomes of which have recently been sequenced (Broad Institute, 2012; Blaxter, 2012), are also heme auxotrophic and must acquire heme from their environment, i.e., the mammalian host. However, it is not known how these filariae actually cover their demand for heme. It is assumed that *Wolbachia* once infected an ancestor common to many filarial nematodes (McNulty et al., 2010) and that *Wolbachia*-free filariae have lost the endosymbiont during evolution. It is conceivable, albeit without experimental verification, that these nematodes became independent of their endosymbionts by developing heme transport machineries that allowed them to exploit exogenous heme sources.

Although it may not be completely ruled out that *Wolbachia*-harboring filarial nematodes may be able to salvage heme from their hosts at least during certain life stages (Attout et al., 2005), the conservation of the heme biosynthetic pathway within the extremely reduced *Wolbachia* genome (Foster et al., 2005) highlights an evolutionary pressure for sustaining this pathway (either for their own supply or for also provisioning to their hosts).

We have previously shown that, upon depletion of >99.8% of *Wolbachia* from the rodent filarial nematode *Ls* by doxycycline, the worms upregulated several mitochondrial encoded heme-dependent subunits of the respiratory chain complexes hypothesized to be a means to overcome the lack of heme supplied by the endosymbiont (Strübing et al., 2010). Treatment of *B. malayi* adult worms with N-methyl mesoporphyrin, a specific ferrochelatase inhibitor, or succinyl acetone (4,6-dioxoheptanoic acid, SA), a non-species-selective inhibitor of ALAD enzymes, led to the death of the worms (Wu et al., 2009). Specificity of the effects of SA is questionable since the high concentration used (3 mM) also affected growth of heme-auxotrophic *C. elegans*. Furthermore, the substrate analog SA undergoes Schiff base formation with a catalytic lysine residue (Erskine et al., 2001) also conserved in the active center of the human ortholog (hALAD) excluding its therapeutic use.

In a high-throughput chemical screen, we have identified a class of specific, small molecule inhibitors, called wALADins, that selectively target the *Wolbachia* ALAD ortholog and exhibit antifilarial activity in vitro. Low μM inhibitory potency in the enzymatic assay and the corresponding high concentrations required to achieve an antifilarial effect against worms in culture make a successful use of these compounds in vivo a challenging but worthy task. The present study paves the way for the development of similar, but more potent, inhibitors (ideally with nanomolar potency) as better drug candidates. These specific inhibitors may further be applied as chemical biology tools to unravel the role of *Wolbachia*-dependent heme biosynthesis in symbiosis and to understand effects caused by depletion with antibiotics (Strübing et al., 2010).

In contrast to previously described ALAD inhibitors, wALADin1 neither acts as a competitive substrate analog nor stabilizes inactive oligomeric assemblies like morphlock inhibitors (Lawrence et al., 2008). wALADin benzimidazoles act by a mixed competitive/noncompetitive mechanism that involves a functional competition with Mg^{2+}. The key to species selectivity lies in the different metal cofactor usage of ALAD families and the corresponding active site architecture and allosteric activation mechanisms. wALAD lacks the cysteine-rich consensus sequence required for Zn^{2+} binding in the catalytic center that is required for catalytic activity by all Zn^{2+}-dependent orthologs (Jaffe, 2003), including the human enzyme. Instead, wALAD is

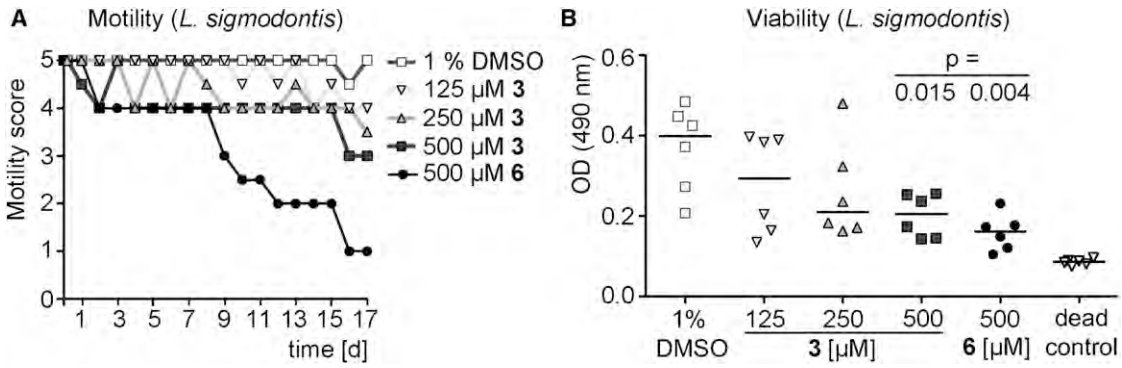

Figure 5. Antifilarial Activity of wAladin Derivatives 3 and 6 against *Ls* In Vitro

(A) *Wolbachia*-containing adult female *Ls* worms treated with 1% DMSO, 125–500 µM **3** or 500 µM **6**. Median values are shown (n = 6).

(B) Worm viability measured by MTT assay at the end of treatment. Significance was tested by nonparametric two-tailed Mann-Whitney U test; significant p values are depicted in the graph. DMSO and dead controls shown in this figure are from the same experiment as in Figure 3.

See also Figure S3 and Movies S1, S2, and S3.

more closely related to the plant (i.e., chloroplast) and several other bacterial orthologs that use Mg^{2+} at the active and/or an allosteric site (Frankenberg et al., 1999; Kervinen et al., 2000; Wu et al., 2009). Despite sporadic evidence for a catalytic active site Mg^{2+} ion substituting the function of the catalytic Zn^{2+} in Zn-dependent orthologs (Kervinen et al., 2000; Petrovich et al., 1996), no crystal structure includes such a Mg^{2+} ion. In contrast, binding of the allosteric Mg^{2+} at a subunit-subunit interface outside the active site is well documented by crystal structures, and the ligand required for binding allosteric Mg^{2+} (Glu_{245} of *P. aeruginosa)* is also conserved in the wALAD protein. Given the monophasic nature of the Mg^{2+} activation profile, we hypothesize that the Mg^{2+} is associated with the well-described allosteric effect, although involvement of active site Mg^{2+} may not be ruled out, given the high affinity binding of Mg^{2+} to the *Wolbachia* ortholog (Kervinen et al., 2000; Shanmugam et al., 2010). wALADin1 may act by competing with Mg^{2+} binding (at either site), or it may bind to a different site and interfere with the allosteric activation process, i.e., allowing closure of the active site lid upon binding of the second 5-ALA substrate to the active site (Frankenberg et al., 1999; Jaffe, 2004). Determination of the binding site of wALADin1 by X-ray crystallography will be required to unravel the molecular mechanism of inhibition. However, efforts to crystallize wALAD have not been successful.

Specific inhibition of wALAD by wALADin1 elicits a macrofilaricidal effect in the living worm in vitro with an IC_{50} of ~100 µM on the *Wolbachia*-harboring *Ls*. In contrast, wALADin1 had little effect on the *Wolbachia*-free *Av*. Thus, the antifilarial activity of wALADin1 is *Wolbachia* dependent. Presumably, this effect results from inhibiting endobacterial heme biosynthesis, although additional targets in *Wolbachia* are possible. The consistent, albeit weaker, antifilarial activity of **3**, a similarly potent wALAD inhibitor according to enzymatic inhibition experiments, supports this conclusion. However, some findings indicate an involvement of a secondary target of wALADins that might act additively or in synergy to inhibit wALAD at high concentrations: (1) the effect of wALADin1 on *Av* motility, (2) cytotoxicity/growth suppression in cell culture above 500 µM, and (3) loss of *Ls* motility and viability by 500 µM **6.**

A potential secondary target may be filarial orthologs of the human Kinesin-spindle protein (hKSP), a potential anticancer drug target required for mitotic spindle assembly. Benzimidazole chemotypes with a substitution pattern similar to that of the wALADins but different in their substituent classes and activity profiles target hKSP and inhibit cancer cell growth (Lahue et al., 2009). The benzimidazole chemotype is also found in anthelminthic compounds like albendazole that target worm β-tubulin (van den Enden, 2009). It has been shown recently that the albendazole metabolite albendazole sulfone targets *Wolbachia* and induces binary fission defects (Serbus et al., 2012). An effect via this still unidentified benzimidazole target is also possible for wALADins, and a detailed elucidation of the *Wolbachia* and filarial phenotypes induced by these compounds is required to unequivocally define the biological effector pathways. However, in light of an ongoing paradigm shift in drug discovery away from single- to multitarget drugs (Hopkins, 2008; Schrattenholz and Soskić, 2008), we are now aiming at the elucidation and exploitation of potential secondary targets of wALADin1 in the development of more potent antifilarial agents.

We have shown that the unique mechanism of ALAD inhibition may already involve a second effector pathway: filarial worms are susceptible to high concentrations of the wALAD substrate 5-ALA; these high concentrations are expected to accumulate when ALAD is inhibited and may mediate pro-oxidative effects and GABA agonism (Brennan and Cantrill, 1979; Warren et al., 1998). GABA agonism itself can lead to a block of neuromuscular activation of nematodes (Martin, 1985). In analogy to pathologic conditions in humans and based on our results, it is possible that, as a consequence to inhibition of wALAD, both 5-ALA toxicity and heme deprivation may contribute in concert to the observed macrofilaricidal effects. The 5-ALA-driven toxicity may even result in an antifilarial effect, in case filarial worms are shown to take up heme from its host under certain conditions. However, the resulting concentrations and the distribution of 5-ALA in *Wolbachia* and in the living worm remain to be determined.

ALAD has been explicitly proposed as a potential drug target in the context of various infectious agents like *Plasmodium*

falciparum (Dhanasekaran et al., 2004), *Toxoplasma gondii* (Shanmugam et al., 2010), and *Pseudomonas aeruginosa* (Frankenberg et al., 1999). The discovery of the ALAD-targeting antibiotic Alaremycin produced by *Streptomyces* (Awa et al., 2005) shows that inhibiting ALAD is a method for antimicrobial killing in nature. Lack of discriminatory power between microbial and mammalian orthologs has been a major drawback for known ALAD inhibitors that may now be overcome with species-selective wALADin benzimidazoles. These Mg^{2+}-competitive inhibitors may be effective against a variety of microbes and plants depending on Mg^{2+}-responsive ALAD function and may be used as antibiotics, herbicides, or antiprotozoal agents.

SIGNIFICANCE

The filarial diseases lymphatic filariasis (lymphedema, hydrocele, and elephantiasis) and onchocerciasis (severe dermatitis and blindness) infect more than 150 million people in developing countries, with 1.2 billion at risk of contracting these diseases. While the distribution of antilarval drugs such as ivermectin or diethylcarbamazine has been used with success in many areas, mathematical modeling has raised questions about the ability of these programs to be efficacious in larger endemic regions. These programs would require 5–20 years of biannual treatment to interrupt transmission, with high costs and uncertain outcome. There are increasing reports on the suboptimal response to ivermectin, the only drug available for onchocerciasis. Therefore, a suitable replacement drug that is effective with a shorter drug regime and that targets the adult worms rather than larval stages is in urgent need. Here, we report a significant step toward such a drug. We have subjected the target δ-aminolevulinic acid dehydratase (ALAD) of *Wolbachia*, essential endobacteria of most filarial parasites of humans, to HTS. We identified a *Wolbachia*-specific inhibitor of ALAD called wALADin1. wALADin1 inhibits via a mixed competitive and noncompetitive mechanism that alters the induction of enzyme activity by Mg^{2+} and has biological activity against the rodent filarial nematode *Litomosoides sigmodontis* in vitro. By synthesizing derivatives of wALADin1, we have identified key chemical motifs required for this inhibitory activity and species selectivity. These compounds are an excellent starting point for the development of antifilarial leads that are urgently needed to achieve final success of lymphatic filariasis and onchocerciasis elimination programs.

EXPERIMENTAL PROCEDURES

Reagents, Proteins, and Enzymatic Assay

The *hemB* gene (ALAD) sequence from wALAD and a cDNA-derived human sequence had been previously cloned into the pET-21a vector (Wu et al., 2009). His6-tagged proteins were expressed with minor changes to the original protocol as described in the Supplemental Experimental Procedures. Metal ion dependencies of the proteins used in this study had been determined in a previous study (Wu et al., 2009), in which specific protein activities had been reported as 57.8 μmol PBG/mg of protein per hour for hALAD and 22.5 μmol PBG/mg of protein per hour for wALAD under optimal buffer conditions. The high-throughput enzymatic screening assay is a simplified standard assay for the detection of PBG with modified Ehrlich's Reagent and is described in detail in Table S1. IC_{50} determinations of inhibitors were performed manually using 500 nM wALAD in 100 mM Tris (pH 8.0) with 5 mM dithiothreitol (DTT), 1 mM $MgCl_2$ or using 250 nM hALAD in 100 mM Tris (pH 7.5) with 5 mM DTT, 10 μM $ZnCl_2$. Ten micromolar of $ZnCl_2$ is a standard concentration used to assay Zn-dependent proteins at optimal activity (Lawrence et al., 2008). Higher levels of Mg^{2+} are required to achieve optimal stimulation. Physiological Mg^{2+} concentrations inside *Wolbachia* are unknown, but free intracellular Mg^{2+} concentrations have been described in the range of 1–10 mM for prokaryotic (Alatossava et al., 1985) and eukaryotic cells (Ebel and Günther, 1980). Protein concentrations were adjusted so that substrate turnover (at 200 μM 5-ALA) after 20 min of reaction at 36°C was 7%–14%. All reagents were purchased from Sigma, Carl Roth, PAA Laboratories, or Life Technologies.

Thermal Shift Assay

Thermal melting curves of ALAD proteins were recorded on a Rotor-Gene RG-3000 (Corbett Life Sciences) in the presence the fluorescent dye SYPRO Orange, which elicits increased fluorescence intensities when bound to hydrophobic amino acids exposed during protein unfolding. Triplicate samples were prepared of 5 μM (0.2 mg/ml) wALAD in 1 M Tris (pH 8.0), 5 mM DTT, 1 mM $MgCl_2$, different concentrations of wALADin1/derivatives or 1% DMSO as control, and 16× SYPRO Orange in a final volume of 10 μl. Control proteins were assayed under identical conditions at 8–16× SYPRO Orange, with chicken egg white lysozyme measured at 3 mg/ml, BSA at 0.5 mg/ml, and hALAD at 0.2 mg/ml in the presence of 10 μM $ZnCl_2$ instead of $MgCl_2$. Samples were denatured with a heating rate of 0.5°C/30 s from 27°C to 95°C. Fluorescence was measured on the FAM (6-carboxyfluorescein) channel (excitation at 470 nm; detection at 510 nm), and first derivative analysis for the measurement analysis was conducted using Rotor-Gene 6 software.

Chemical Compounds and Syntheses

See full methods in Supplemental Experimental Procedures for the detailed synthesis.

Animals, Infections, Cells, and Coculture Assays

Protocol approval and ethical clearance for animal handling was obtained from the Landesamt für Natur Umwelt und Verbraucherschutz Nordrhein Westfalen in Recklinghausen, Germany (AZ 8.87-50.10.35.08.024). German and European Union guidelines to minimize animal suffering were followed. *Av*-infected Mongolian gerbils were kindly provided by Dr. R. Lucius (Humboldt-Universität zu Berlin, Berlin, Germany).

The *Ls* cycle was maintained at the University Hospital of Bonn (Bonn, Germany) as previously described (Al-Qaoud et al., 1997). For natural infection with *Ls*, anesthetized gerbils were exposed to tropical dust mites (*Ornithonyssus bacoti*) infected with *Ls*. Patently infected animals were euthanized after 3–9 months postinfection, and adult *Ls* worms were isolated from the pleural cavity. *Av* were isolated from the subcutaneous tissue of gerbils 6–12 months after infection. Isolated adult female worms of *Ls* or *Av* were washed and placed on a confluent lawn of LLC-MK2 cells (a kind gift of S. Townson, London School of Hygiene and Tropical Medicine) in six-well plates (six worms per group) and kept at 37°C, 5% CO_2. After 24 hr, worms were exposed to the drugs or 1% DMSO control in 3 ml medium for 14–17 days. Medium was exchanged every 2 days. Please refer to Supplemental Experimental Procedures for a description of the motility scores and worm viability measurements by MTT assay adapted from a study initially describing the coculture system for male adults of another filarial species (Townson et al., 2006).

Statistics and Data Analyses

All data and statistics were analyzed using Prism 5.0 (GraphPad Software). Results of enzymatic assays are given as the mean ± SEM. Curves were fitted using the "$\log_{inhibitor}$ versus normalized response – variable slope" nonlinear regression algorithm. Hill-slope values were allowed to adopt values different from −1 due to the possibility of different cooperative effects on ALAD oligomers. Predicted Hill-slope values ranged from −0.45 to −0.81. For type-of-inhibition experiments, primary data were fitted using the mixed model inhibition algorithm and linear Eadie-Hofstee representations were generated. Statistical analyses were conducted using the nonparametric two-tailed Mann-Whitney U test for significance testing with a significance level of $\alpha = 0.05$.

SUPPLEMENTAL INFORMATION

Supplemental Information includes four figures, one table, five movies, and Supplemental Experimental Procedures and can be found with this article online at http://dx.doi.org/10.1016/j.chembiol.2012.11.009.

ACKNOWLEDGMENTS

We thank B. Slatko and B. Wu of New England Biolabs for the wALAD and hALAD expression plasmids and for help with enzyme expression, purification, and activity measurement; S. Townson for LLC-MK2 cells; R. Lucius for *Av*-infected Mongolian gerbils; K. Rotscheidt and K. Gorski-Rzepinski for excellent technical assistance; and the members of the Famulok and Hoerauf laboratories. We also thank M. Blaxter and G. Koutsovoulos, University of Edinburgh, who sequenced and assembled the *Av* genome with funding from the European Commission as part of the Enhanced Protective Immunity against Filariasis Consortium (Contract No. 242131), and E.K. Jaffe for helpful discussions. This work was supported through a grant from the Liverpool School of Tropical Medicine to A.H. and K.M.P. as part of the A-WOL (Anti-*Wolbachia*) Consortium funded by the Bill and Melinda Gates Foundation; the BONFOR intramural funding program to A.H.; and the Deutsche Forschungsgemeinschaft (SFB 704) and the North Rhine Westfalia research school Life and Medical Sciences Institute (LIMES)—Chemical Biology to M.F.

Received: September 27, 2012
Revised: November 19, 2012
Accepted: November 21, 2012
Published: February 21, 2013

REFERENCES

Al-Qaoud, K.M., Taubert, A., Zahner, H., Fleischer, B., and Hoerauf, A. (1997). Infection of BALB/c mice with the filarial nematode Litomosoides sigmodontis: role of CD4+ T cells in controlling larval development. Infect. Immun. *65*, 2457–2461.

Alatossava, T., Jütte, H., Kuhn, A., and Kellenberger, E. (1985). Manipulation of intracellular magnesium content in polymyxin B nonapeptide-sensitized Escherichia coli by ionophore A23187. J. Bacteriol. *162*, 413–419.

Attout, T., Babayan, S., Hoerauf, A., Taylor, D.W., Kozek, W.J., Martin, C., and Bain, O. (2005). Blood-feeding in the young adult filarial worms Litomosoides sigmodontis. Parasitology *130*, 421–428.

Awa, Y., Iwai, N., Ueda, T., Suzuki, K., Asano, S., Yamagishi, J., Nagai, K., and Wachi, M. (2005). Isolation of a new antibiotic, alaremycin, structurally related to 5-aminolevulinic acid from Streptomyces sp. A012304. Biosci. Biotechnol. Biochem. *69*, 1721–1725.

Blaxter, M.L. (2012). The genome of the filarial nematode Acanthocheilonema viteae. http://nematodes.org/genomes/acanthocheilonema_viteae

Bockarie, M.J., and Deb, R.M. (2010). Elimination of lymphatic filariasis: do we have the drugs to complete the job? Curr. Opin. Infect. Dis. *23*, 617–620.

Bourguinat, C., Keller, K., Blagburn, B., Schenker, R., Geary, T.G., and Prichard, R.K. (2011). Correlation between loss of efficacy of macrocyclic lactone heartworm anthelmintics and P-glycoprotein genotype. Vet. Parasitol. *176*, 374–381.

Brennan, M.J., and Cantrill, R.C. (1979). Delta-aminolaevulinic acid is a potent agonist for GABA autoreceptors. Nature *280*, 514–515.

Broad Institute. (2012). Filarial worms database: project information. http://www.broadinstitute.org/annotation/genome/filarial_worms/MultiHome.html

Chen, C., Samuel, T.K., Krause, M., Dailey, H.A., and Hamza, I. (2012). Heme utilization in the Caenorhabditis elegans hypodermal cells is facilitated by heme-responsive gene-2. J. Biol. Chem. *287*, 9601–9612.

Churcher, T.S., Pion, S.D., Osei-Atweneboana, M.Y., Prichard, R.K., Awadzi, K., Boussinesq, M., Collins, R.C., Whitworth, J.A., and Basáñez, M.G. (2009). Identifying sub-optimal responses to ivermectin in the treatment of River Blindness. Proc. Natl. Acad. Sci. USA *106*, 16716–16721.

Dhanasekaran, S., Chandra, N.R., Chandrasekhar Sagar, B.K., Rangarajan, P.N., and Padmanaban, G. (2004). Delta-aminolevulinic acid dehydratase from Plasmodium falciparum: indigenous versus imported. J. Biol. Chem. *279*, 6934–6942.

Ebel, H., and Günther, T. (1980). Magnesium metabolism: a review. J. Clin. Chem. Clin. Biochem. *18*, 257–270.

Erskine, P.T., Newbold, R., Brindley, A.A., Wood, S.P., Shoolingin-Jordan, P.M., Warren, M.J., and Cooper, J.B. (2001). The x-ray structure of yeast 5-aminolaevulinic acid dehydratase complexed with substrate and three inhibitors. J. Mol. Biol. *312*, 133–141.

Esterre, P., Plichart, C., Sechan, Y., and Nguyen, N.L. (2001). The impact of 34 years of massive DEC chemotherapy on Wuchereria bancrofti infection and transmission: the Maupiti cohort. Trop. Med. Int. Health *6*, 190–195.

Foster, J., Ganatra, M., Kamal, I., Ware, J., Makarova, K., Ivanova, N., Bhattacharyya, A., Kapatral, V., Kumar, S., Posfai, J., et al. (2005). The Wolbachia genome of Brugia malayi: endosymbiont evolution within a human pathogenic nematode. PLoS Biol. *3*, e121.

Frankenberg, N., Heinz, D.W., and Jahn, D. (1999). Production, purification, and characterization of a Mg2+-responsive porphobilinogen synthase from Pseudomonas aeruginosa. Biochemistry *38*, 13968–13975.

Gardon, J., Gardon-Wendel, N., Demanga-Ngangue, Kamgno, J., Chippaux, J.P., and Boussinesq, M. (1997). Serious reactions after mass treatment of onchocerciasis with ivermectin in an area endemic for Loa loa infection. Lancet *350*, 18–22.

Geary, T.G., and Mackenzie, C.D. (2011). Progress and challenges in the discovery of macrofilaricidal drugs. Expert Rev. Anti Infect. Ther. *9*, 681–695.

Ghedin, E., Wang, S., Spiro, D., Caler, E., Zhao, Q., Crabtree, J., Allen, J.E., Delcher, A.L., Guiliano, D.B., Miranda-Saavedra, D., et al. (2007). Draft genome of the filarial nematode parasite Brugia malayi. Science *317*, 1756–1760.

Global programme to eliminate lymphatic filariasis. (2009). Wkly. Epidemiol. Rec. *84*, 437–444.

Global programme to eliminate lymphatic filariasis: progress report on mass drug administration, 2010. (2011). Wkly. Epidemiol. Rec. *86*, 377–388.

Gloeckner, C., Garner, A.L., Mersha, F., Oksov, Y., Tricoche, N., Eubanks, L.M., Lustigman, S., Kaufmann, G.F., and Janda, K.D. (2010). Repositioning of an existing drug for the neglected tropical disease Onchocerciasis. Proc. Natl. Acad. Sci. USA *107*, 3424–3429.

Hafner, M., Schmitz, A., Grüne, I., Srivatsan, S.G., Paul, B., Kolanus, W., Quast, T., Kremmer, E., Bauer, I., and Famulok, M. (2006). Inhibition of cytohesins by SecinH3 leads to hepatic insulin resistance. Nature *444*, 941–944.

Hafner, M., Vianini, E., Albertoni, B., Marchetti, L., Grüne, I., Gloeckner, C., and Famulok, M. (2008). Displacement of protein-bound aptamers with small molecules screened by fluorescence polarization. Nat. Protoc. *3*, 579–587.

Hoerauf, A., Nissen-Pähle, K., Schmetz, C., Henkle-Dührsen, K., Blaxter, M.L., Büttner, D.W., Gallin, M.Y., Al-Qaoud, K.M., Lucius, R., and Fleischer, B. (1999). Tetracycline therapy targets intracellular bacteria in the filarial nematode Litomosoides sigmodontis and results in filarial infertility. J. Clin. Invest. *103*, 11–18.

Hoerauf, A., Volkmann, L., Hamelmann, C., Adjei, O., Autenrieth, I.B., Fleischer, B., and Büttner, D.W. (2000). Endosymbiotic bacteria in worms as targets for a novel chemotherapy in filariasis. Lancet *355*, 1242–1243.

Hoerauf, A., Specht, S., Marfo-Debrekyei, Y., Büttner, M., Debrah, A.Y., Mand, S., Batsa, L., Brattig, N., Konadu, P., Bandi, C., et al. (2009). Efficacy of 5-week doxycycline treatment on adult Onchocerca volvulus. Parasitol. Res. *104*, 437–447.

Hoerauf, A., Pfarr, K., Mand, S., Debrah, A.Y., and Specht, S. (2011). Filariasis in Africa—treatment challenges and prospects. Clin. Microbiol. Infect. *17*, 977–985.

Hopkins, A.L. (2008). Network pharmacology: the next paradigm in drug discovery. Nat. Chem. Biol. *4*, 682–690.

Jaffe, E.K. (2003). An unusual phylogenetic variation in the metal ion binding sites of porphobilinogen synthase. Chem. Biol. *10*, 25–34.

Jaffe, E.K. (2004). The porphobilinogen synthase catalyzed reaction mechanism. Bioorg. Chem. *32*, 316–325.

Jaffe, E.K. (2005). Morpheeins—a new structural paradigm for allosteric regulation. Trends Biochem. Sci. *30*, 490–497.

Kervinen, J., Dunbrack, R.L., Jr., Litwin, S., Martins, J., Scarrow, R.C., Volin, M., Yeung, A.T., Yoon, E., and Jaffe, E.K. (2000). Porphobilinogen synthase from pea: expression from an artificial gene, kinetic characterization, and novel implications for subunit interactions. Biochemistry *39*, 9018–9029.

Lahue, B.R., Ma, Y., Shipps, G.W., Jr., Seghezzi, W., and Herbst, R. (2009). Substituted benzimidazoles: A novel chemotype for small molecule hKSP inhibitors. Bioorg. Med. Chem. Lett. *19*, 3405–3409.

Lawrence, S.H., Ramirez, U.D., Tang, L., Fazliyez, F., Kundrat, L., Markham, G.D., and Jaffe, E.K. (2008). Shape shifting leads to small-molecule allosteric drug discovery. Chem. Biol. *15*, 586–596.

Martin, R.J. (1985). gamma-Aminobutyric acid- and piperazine-activated single-channel currents from Ascaris suum body muscle. Br. J. Pharmacol. *84*, 445–461.

McNulty, S.N., Foster, J.M., Mitreva, M., Dunning Hotopp, J.C., Martin, J., Fischer, K., Wu, B., Davis, P.J., Kumar, S., Brattig, N.W., et al. (2010). Endosymbiont DNA in endobacteria-free filarial nematodes indicates ancient horizontal genetic transfer. PLoS ONE *5*, e11029.

Niebel, B., Lentz, C., Pofahl, M., Mayer, G., Hoerauf, A., Pfarr, K.M., and Famulok, M. (2010). ADLOC: an aptamer-displacement assay based on luminescent oxygen channeling. Chemistry *16*, 11100–11107.

Osei-Atweneboana, M.Y., Awadzi, K., Attah, S.K., Boakye, D.A., Gyapong, J.O., and Prichard, R.K. (2011). Phenotypic evidence of emerging ivermectin resistance in Onchocerca volvulus. PLoS Negl. Trop. Dis. *5*, e998.

Petrovich, R.M., Litwin, S., and Jaffe, E.K. (1996). Bradyrhizobium japonicum porphobilinogen synthase uses two Mg(II) and monovalent cations. J. Biol. Chem. *271*, 8692–8699.

Schrattenholz, A., and Soskić, V. (2008). What does systems biology mean for drug development? Curr. Med. Chem. *15*, 1520–1528.

Serbus, L.R., Landmann, F., Bray, W.M., White, P.M., Ruybal, J., Lokey, R.S., Debec, A., and Sullivan, W. (2012). A cell-based screen reveals that the albendazole metabolite, albendazole sulfone, targets Wolbachia. PLoS Pathog. *8*, e1002922.

Shanmugam, D., Wu, B., Ramirez, U., Jaffe, E.K., and Roos, D.S. (2010). Plastid-associated porphobilinogen synthase from Toxoplasma gondii: kinetic and structural properties validate therapeutic potential. J. Biol. Chem. *285*, 22122–22131.

Slatko, B.E., Taylor, M.J., and Foster, J.M. (2010). The Wolbachia endosymbiont as an anti-filarial nematode target. Symbiosis *51*, 55–65.

Strübing, U., Lucius, R., Hoerauf, A., and Pfarr, K.M. (2010). Mitochondrial genes for heme-dependent respiratory chain complexes are up-regulated after depletion of Wolbachia from filarial nematodes. Int. J. Parasitol. *40*, 1193–1202.

Taylor, M.J., Bandi, C., and Hoerauf, A. (2005). Wolbachia bacterial endosymbionts of filarial nematodes. Adv. Parasitol. *60*, 245–284.

Taylor, M.J., Hoerauf, A., and Bockarie, M. (2010). Lymphatic filariasis and onchocerciasis. Lancet *376*, 1175–1185.

Townson, S., Tagboto, S., McGarry, H.F., Egerton, G.L., and Taylor, M.J. (2006). Onchocerca parasites and Wolbachia endosymbionts: evaluation of a spectrum of antibiotic types for activity against Onchocerca gutturosa in vitro. Filaria J. *5*, 4.

van den Enden, E. (2009). Pharmacotherapy of helminth infection. Expert Opin. Pharmacother. *10*, 435–451.

Warren, M.J., Cooper, J.B., Wood, S.P., and Shoolingin-Jordan, P.M. (1998). Lead poisoning, haem synthesis and 5-aminolaevulinic acid dehydratase. Trends Biochem. Sci. *23*, 217–221.

Wu, B., Novelli, J., Foster, J., Vaisvila, R., Conway, L., Ingram, J., Ganatra, M., Rao, A.U., Hamza, I., and Slatko, B. (2009). The heme biosynthetic pathway of the obligate Wolbachia endosymbiont of Brugia malayi as a potential anti-filarial drug target. PLoS Negl. Trop. Dis. *3*, e475.

Yamazaki, S., Tan, L., Mayer, G., Hartig, J.S., Song, J.N., Reuter, S., Restle, T., Laufer, S.D., Grohmann, D., Kräusslich, H.G., et al. (2007). Aptamer displacement identifies alternative small-molecule target sites that escape viral resistance. Chem. Biol. *14*, 804–812.

Zhang, R., and Monsma, F. (2010). Fluorescence-based thermal shift assays. Curr. Opin. Drug Discov. Devel. *13*, 389–402.